Materials Science and Engineering C 40 (2014) 42–48

Contents lists available at ScienceDirect

Materials Science and Engineering C

journal homepage: www.elsevier.com/locate/msec

Preparation of mesoporous silica thin films by photocalcination method and their adsorption abilities for various proteins

Katsuya Kato [a,*], Hitomi Nakamura [a], Yoshihiro Yamauchi [b], Kazuma Nakanishi [b], Masahiro Tomita [b]

[a] National Institute of Advanced Industrial Science and Technology (AIST), 2266-98 Anagahora, Shimoshidami, Moriyama-ku, Nagoya 463-8560, Japan
[b] Department of Chemistry for Materials, Graduate School of Engineering, Mie University, 1577 Kurimamachiya-cho, Tsu, Mie 514-8570, Japan

ARTICLE INFO

Article history:
Received 30 January 2014
Received in revised form 25 February 2014
Accepted 18 March 2014
Available online 26 March 2014

Keywords:
Mesoporous silica
Thin film
Protein A
Antibody
ELISA

ABSTRACT

Mesoporous silica (MPS) thin film biosensor platforms were established. MPS thin films were prepared from tetraethoxysilane (TEOS) via using sol–gel and spin-coating methods using a poly-(ethylene oxide)-block-poly-(propylene oxide)-block-poly-(ethylene oxide) triblock polymer, such as P123 ($(EO)_{20}(PO)_{70}(EO)_{20}$) or F127 ($(EO)_{106}(PO)_{70}(EO)_{106}$), as the structure-directing agent. The MPS thin film prepared using P123 as the mesoporous template and treated via vacuum ultraviolet (VUV) irradiation to remove the triblock copolymer had a more uniform pore array than that of the corresponding film prepared via thermal treatment. Protein adsorption and enzyme-linked immunosorbent assay (ELISA) on the synthesized MPS thin films were also investigated. VUV-irradiated MPS thin films adsorbed a smaller quantity of protein A than the thermally treated films; however, the human immunoglobulin G (IgG) binding efficiency was higher on the former. In addition, protein A–IgG specific binding on MPS thin films was achieved without using a blocking reagent; i.e., nonspecific adsorption was inhibited by the uniform pore arrays of the films. Furthermore, VUV-irradiated MPS thin films exhibited high sensitivity for ELISA testing, and cytochrome c adsorbed on the MPS thin films exhibited high catalytic activity and recyclability. These results suggest that MPS thin films are attractive platforms for the development of novel biosensors.

1. Introduction

Mesoporous silica (MPS) was developed in 1990 by Kuroda et al. [1,2], and the sol–gel method for its preparation was reported by researchers at Mobil Co. in 1992 [3]. MPS is a nanomaterial with a uniform pore diameter in the range 2–50 nm, a high specific surface area, and a high pore volume [4,5]. The structure of MPS, including its composition, orientation, diameter, pore volume, and surface area, can be controlled by using structure-directing agents such as surfactants and triblock copolymers. For this reason, MPS is promising as an adsorption material, catalyst carrier, and separation sensor. In addition, biological applications such as drug delivery systems, transfect ion devices, and regenerative medicines are expected to be developed based on MPS. We previously reported the encapsulation of biomolecules on MPS particles for use in biological applications such as biocatalysis and bioaffinity chromatography [6,7]. These MPS particles, which have regular structures with pore sizes 3–40 nm, were synthesized via a sol–gel method. The immobilization of enzymes and antibodies on MPS particles has also been investigated, e.g., Yang et al. used MPS particles to develop electrochemical immunosensors [8] based on functionalized MPS nanoparticles that were shown to be effective for the ultrasensitive detection of low concentrations of antigens (0.01–10 ng/mL). In addition, MPS thin films have also been prepared via the sol–gel method or using dip- and spin-coating techniques. The spin-coating method is particularly suited for the development of industrial methods because the film thickness can be controlled by varying the viscosity of the coating solution and the rate of spin coating. Therefore, MPS thin films have a potential for use in optical devices, gas sensors, separation membranes, and adsorption materials [9–12].

Biosensor is a generic term for chemical sensors that rely on molecular recognition using biological materials. The biosensor concept was first proposed in 1962 by Clark and first reported in 1967 by Updike and Hicks [13]. This report described a sensor that indicated the presence or absence of glucose using a glucose oxidase-supported electrode that detected the generation of hydrogen peroxide (H_2O_2). Since then, many biosensors have been developed, such as those that utilize the responses of enzymes and antibodies and those that convert biological reactions into electronic signals, e.g., a glucose sensor based on immobilized glucose oxidase is used as an autological blood glucose monitoring sensor for diabetic patients [14–17]. In the environmental field, biological oxygen demand sensors based on immobilized microbes have been commercialized and used for monitoring discharged water and the determining the extent of water pollution [18]. In recent years, biosensors have been applied as measurement devices in a growing number of fields, and it is

* Corresponding author at: 2266-98 Anagahora, Shimoshidami, Moriyama, Nagoya, 463-8560, Japan. Tel.: +81 52 736 7551; fax: +81 52 736 7405.
E-mail address: katsuya-kato@aist.go.jp (K. Kato).

http://dx.doi.org/10.1016/j.msec.2014.03.045
0928-4931/

now possible to achieve both selective and simple measurements. The uniform mesopore array of MPS thin films is expected to enable the development of highly sensitive biosensors; however, to the best of our knowledge, the development of biosensing systems based on MPS thin films has not yet been reported. Therefore, the investigation of protein adsorption on MPS thin films is very attractive as a potential approach to the development of novel biosensors.

Cytochrome c (cyt c) is one of the most extensively studied eukaryotic proteins, and it is synthesized in the cytoplasm. It is a redox-active heme protein (molecular size 2.5 × 2.5 × 3.7 nm, MW 12 kDa) consisting of 104 amino acid residues. The active heme center of cyt c consists of a porphyrin ring in which the four pyrrole nitrogens are coordinated to the Fe atom, forming a square planar complex. The iron center switches between the ferric (Fe^{3+}) and the ferrous (Fe^{2+}) state, thus acting as an electron carrier. Posttranslational addition of the cyt c heme moiety is catalyzed by heme lyase in the inner membrane space of the mitochondria [19–21]. Biosensors based on immobilized cyt c as an electron carrier have been reported for the detection of organophosphorus and for use as electrodes [22–24]. Such biosensors have several advantages, including simple fabrication, fast response, and high stability. Importantly, commercial use of cyt c on MPS thin films as sensors and catalysts has been rarely reported.

Herein, we describe the preparation and use of MPS thin films as platforms for biosensors. MPS thin films were prepared via spin coating, and their use in biosensors was investigated. Specifically, the relationship between the mesoporous structures of the MPS thin films and the sensitivity of the developed biosensors was evaluated because both the pore size and array structure of the thin films are major factors determining the sensitivity of such biosensors. Therefore, understanding the effect of the mesoporous structure should enable the preparation of novel, highly sensitive biosensor platforms. In addition, protein adsorption on the MPS thin films was investigated via dynamic force microscopy, and enzyme-linked immunosorbent assay (ELISA) and catalytic reactions of cyt c as a model biocatalyst on the MPS thin films were also performed.

2. Materials and methods

2.1. Materials

All materials were analytical grade and used as received without further purification. Ethanol (EtOH) and H_2O_2 were procured from Wako Pure Chemical Industries, Tokyo, Japan. The triblock copolymer P123 (Mw = 5800, $(EO)_{20}(PO)_{70}(EO)_{20}$; EO = ethylene oxide, PO = propylene oxide), protein A (from *Staphylococcus aureus*, catalog number P6031; molecular weight = 42 kDa; isoelectric point (pI) = 5.1; molecular size = approximately 3 nm), human immunoglobulin G (IgG) conjugated with fluorescein isothiocyanate (FITC–IgG, catalog number F9636; molecular weight = 150 kDa; isoelectric point (pI) = 10.0–10.5; molecular size = 7 nm × 19 nm × 7 nm), a fluoroprofile protein quantification kit (FP0010), and cyt c (from equine heart, catalog number C7752; molecular weight = 12 kDa; isoelectric point (pI) = 10.0–10.5; molecular size = 2.6 nm × 3.2 nm × 3.3 nm) were purchased from Sigma-Aldrich (St. Louis, MO, USA). Triblock polymer F127 (Mw = 12500, $(EO)_{106}(PO)_{70}(EO)_{106}$) was obtained from BASF Japan (Tokyo, Japan). Tetraethoxysilane (TEOS) was obtained from Shin-Etsu Chemical Co., Tokyo, Japan. Hydrochloric acid (HCl) was purchased from Kanto Chemical Co. Inc., Tokyo, Japan. A human IgG ELISA quantitation kit was obtained from BETHYL (Montgomery, AL, USA). The compound 2,2′-azino-bis(3-ethylbenzothiazoline-6-sulfonic acid) (ABTS) was acquired from Tokyo Chemical Industry Co., Tokyo, Japan. A superblock blocking buffer (SBBB, No. 37535) in Tris-buffered saline (TBS) was obtained from Pierce, Rockford, IL, USA. This blocking reagent was used for the prevention of the nonspecific adsorption of human reference serum (antigen) during the ELISA experiments.

2.2. Preparation of the sol–gel solutions

MPS thin films were prepared from sol–gel solutions using a spin-coating method. Three types of silica sol solutions were prepared: P123-sol, F127-sol, and Silica-sol. P123-sol and F127-sol were prepared via the addition of P123 and F127 as mesoporous organic templates, respectively, and the Silica-sol was prepared without using an organic template. Templates with different molecular weights were employed in order to investigate the performance of MPS thin films with different mesopore diameters. First, a polymer solution was prepared by dissolving a triblock copolymer (P123 or F127) in ethanol with stirring for 2 h at 25 °C. A silica precursor solution was prepared separately by mixing TEOS, HCl (10 M), and EtOH for 2 h in another vessel. Next, each polymer solution was mixed with the silica precursor solution and stirred for another 2 h. The three types of sol solutions that were prepared were as follows:

i) P123-sol: P123, 1.0 g; TEOS, 3.9 g; EtOH, 32.9 g; H_2O, 5.1 g; 10 M HCl, 0.3 mL.
ii) F127-sol: F127, 1.0 g; TEOS, 4.1 g; EtOH, 34.5 g; H_2O, 5.3 g; 10 M HCl, 0.3 mL.
iii) Silica-sol: TEOS, 3.9 g; EtOH, 32.9 g; H_2O, 5.1 g; 10 M HCl, 0.3 mL.

2.3. Synthesis of MPS thin films

MPS thin films were prepared via spin-coating of the sol solutions described above. The MPS thin films were coated on slide glass substrates (ϕ 15 mm) that were first cleaned via UV irradiation at 1.3×10^{-3} Pa for 15 min using an eximer UER20-172V UV lamp (Ushio, Inc., Tokyo, Japan; light source: Xe lamp; wavelength: 172 nm; light intensity: 10 mW/cm^2). Each cleaned slide was dripped with 150 μL of each sol solution, and the slides were spin-coated first at 500 rpm for 5 s and then at 3000 rpm for 30 s. The coated glass slides were then dried at 80 °C for 3 h in order to enable evaporation-induced self-assembly (EISA) [25,26]. Finally, the organic template polymers were removed by calcining at 500 °C for 3 h or via vacuum UV (VUV) treatment at 1.3×10^{-3} Pa for 1 h [27]. The thin films prepared using the Silica-sol, P123-sol, and F127-sol is referred to as Silica-F, P123-F, and F127-F, respectively. In addition, VUV irradiation and thermal treatment are abbreviated as V and T, respectively, e.g., P123-FV refers to the thin film prepared from the P123-sol and subjected to VUV irradiation, while P123-FT refers to the thin film prepared from the P123-sol and calcined at 500 °C. P123-FN indicated the as-made film prior to the removal of the polymer.

2.4. Characterization of the MPS thin films

All of the prepared MPS thin films were characterized using a small-angle X-ray diffractometer (XRD, RINT2100V/PC, Rigaku, Tokyo, Japan) (Fe-Kα, 40 kV, 30 mA) over a scanning range 0.6°–12° (2θ). The hydrophilic properties of the MPS thin films were evaluated via measurement of the contact angle using a CA-X (Kyowa Interface Science Co., Tokyo, Japan). Dynamic force microcopy (DFM, scanning probe microscope (SPM), SPA-400, SII NanoTechnology Inc., Tokyo, Japan) was used to investigate the surface characteristics of each of the MPS thin film, such as the surface area and root mean square (RMS) roughness. An area of 2 μm × 2 μm was scanned using a 110 μm scanner and an SI-DF20 cantilever (SII NanoTechnology Inc.). The thickness of the MPS thin films was determined based on ellipsometry measurements obtained using a M2000 ellipsometer (J.A. Woollam Co. Inc., Lincoln, NE, USA) at room temperature over the energy (E) range 0.7–5.0 eV using light with angles of incidence to the films of 50°, 60°, and 70° [28–30]. Protein adsorption on the MPS particles was confirmed by analyzing the nitrogen gas adsorption/desorption isotherms and pore distributions of the mesoporous silica particles at 77 K obtained using a TriStar 3000 system (Shimadzu Co., Kyoto, Japan). MPS particles

prepared via hydrothermal treatment at 130 °C for 3 days were found to have a composition similar to that of the P123-sol.

2.5. Protein adsorption on the MPS thin films

Protein adsorption on the MPS thin films was performed using protein A and FITC–IgG [31–33]. MPS thin films were placed in 24 well plates, protein A solution (40 μg/500 μL) dissolved in 10 mM phosphate buffer solution (500 μL, pH 7.0) was then added to each well, and the solutions were gently stirred overnight at room temperature. Using the fluoroprofile fluorescence reagent, the amount of protein remaining in the supernatant was then determined by measuring the excitation/fluorescence band at 355 nm/615 nm with a fluorescence spectrometer (RF-5300PC, Shimadzu Co., Kyoto, Japan). The amount of adsorbed protein on the MPS thin films was then calculated using the quantity of protein detected in the supernatant.

The MPS thin films with adsorbed protein A (after the removal of the remaining unadsorbed protein) were then treated with FITC–IgG. An FITC–IgG (10 μg/500 μL) solution was prepared by dissolving the FITC–IgG in 10 mM phosphate buffer solution (500 μL, pH 7.0), and then this solution was added to each well containing the MPS thin films with adsorbed protein A. The well plate was gently shaken in the dark for 3 h at room temperature, and then the amount of FITC–IgG remaining in the supernatant was determined by measuring the fluorescence intensities at 485 nm and 535 nm using a fluorescence spectrometer.

2.6. ELISA tests on the MPS thin films

ELISA tests using a human IgG ELISA quantitation kit [34–36] were performed in order to investigate the application of MPS thin films as biosensors. The ELISA testing process on the MPS thin films is illustrated in Scheme S1. First, the MPS thin films were placed in a 24 well plate, and a protein A solution (40 μg/500 μL) was added to each well (Scheme S1a). After stirring for 6 h at room temperature, supernatant from each well was removed, and each MPS thin film was washed three times with antibody washing solution (0.1% Tween 20 in 10 mM, pH 7.4 phosphate buffer solution). Next, an antibody coating solution (10 μg/500 μL) as the primary antibody was added to each well, and the solutions were stirred for 12 h at room temperature (Scheme S1b). Each MPS thin film was then washed three times with antibody washing solution, and subsequently superblock blocking buffer (SBBB, 500 μL) was added to inhibit nonspecific adsorption. After stirring for 3 h at room temperature, the MPS thin films were washed five times with antibody washing solution, and then an antigen solution (500 μL) with a concentration range 3.9–250 ng/500 μL was placed into each well (Scheme S1c). After gently shaking for 1 h, the MPS thin films were again rinsed five times with an antibody washing solution and then supplied with a horseradish peroxidase (HRP) conjugated antibody solution (10 μg/500 μL) as a secondary antibody. The secondary antibody was allowed to react with the antigen on the MPS thin films for 1 h (Scheme S1d), and then the MPS thin films were rinsed five times. Subsequently, a tetramethylbenzidine solution (500 μL, 0.1 mg/mL 10 mM phosphate buffer pH 6.5) was added to each well, and the solutions were stirred for 10 min in the dark at room temperature (Scheme S1e). Finally, 80 μL of the supernatant in each well and 20 μL of 1 M sulfuric acid were mixed in 96 well plates, and the mixtures were evaluated using a UV–vis spectrophotometer (V-560, Jasco Co., Tokyo, Japan) at a wavelength of 450 nm.

2.7. Catalytic activity of cyt c on the MPS thin films

The potential for application of the MPS thin films as biosensors based on catalytic activity was investigated using cyt c. The peroxidase activity of cyt c was measured using ABTS and H_2O_2. ABTS is water soluble and has a strong absorption band at 340 nm [37], while its oxidized derivative is blue-green in color and its absorption band is shifted to 420 nm. First, cyt c (50 μg) was adsorbed onto the MPS thin films using a procedure similar to that described in protein adsorption on the MPS thin films. The MPS thin films with adsorbed cyt c were placed into a 24 well plate; 10 mM phosphate buffer solution (pH 7.0), ABTS (50 μM), and 0.3 μM H_2O_2 were added to reach a total volume of 700 μL in each well; then the cyt c on the MPS thin films was allowed to react for 10 min at room temperature. Subsequently, the absorbance at 420 nm for each reaction mixture was measured using a UV–vis spectrophotometer. In addition, a reaction mixture without cyt c was prepared as a blank, and its absorbance was measured at 420 nm. The specific activity of cyt c on the films was calculated using the following equation:

$$\text{Specific activity} = (\Delta_A - \Delta_B)/t/w \quad (1)$$

where Δ_A is the absorbance of the reaction with cyt c, Δ_B is the absorbance of the reaction without cyt c, t is the reaction time (min), and w is the amount of cyt c on the film (μg).

The recyclability of cyt c on the films was also determined using a similar procedure. As a positive control, the specific activity of a free cyt c solution was evaluated using the same procedure. Each reported value is the mean of the results obtained for at least three experiments.

3. Results and discussion

3.1. Characterization of synthesized MPS thin films

XRD patterns and the d_{100} spacings of each MPS thin film are shown in Fig. 1. P123-FN had a sharp peak in its XRD pattern at $2\theta = 1.4°$ and a *d* spacing of 7.9 nm. After VUV or thermal treatment, P123-FV exhibited a peak at $2\theta = 2.0°$ in its XRD pattern with a *d* spacing of 5.0 nm, while P123-FT exhibited a broad peak at $2\theta = 2.2°$ in its XRD pattern with a *d*

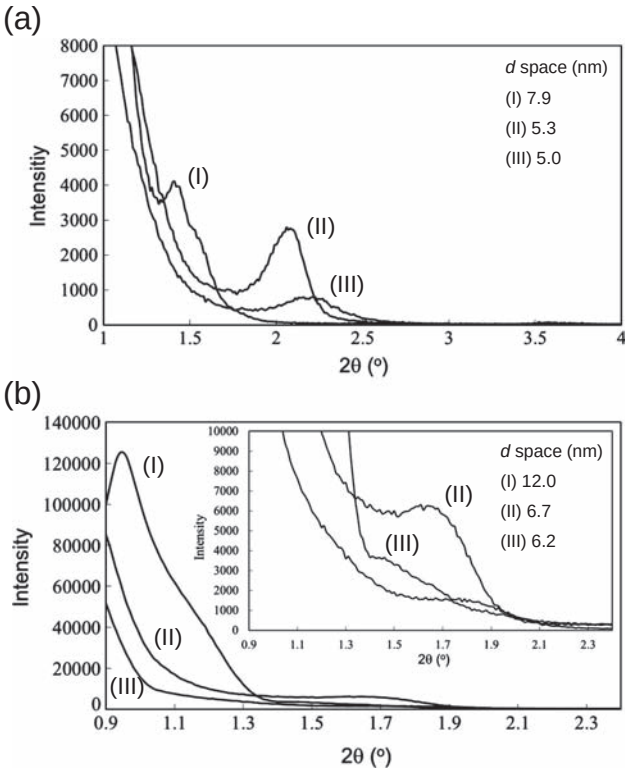

Fig. 1. X-ray diffractometer (XRD) patterns of mesoporous silica (MPS) thin films prepared via vacuum ultraviolet (VUV) and thermal treatment. MPS thin films using (a) P123 (P123-F) and (b) F127 (F127-F). (I) As-made films, (II) VUV treatment, and (III) thermal treatment.

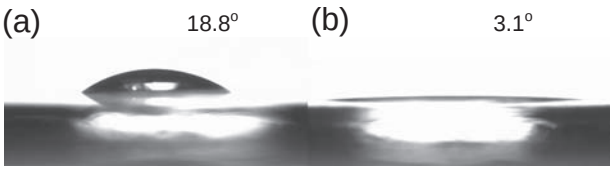

Fig. 2. Contact angles of mesoporous silica (MPS) thin films prepared via vacuum ultraviolet (VUV) and thermal treatment. (a) P123-FT and (b) P123-FV.

spacing of 5.3 nm, respectively (Fig. 1a). Meanwhile, the XRD patterns of the F127 thin films (F127-FN, F127-FV, and F127-T) exhibited peaks at $2\theta = 0.95°$ (d spacing = 12.0 nm), 1.6° (6.2 nm), and 1.5° (6.7 nm), respectively (Fig. 1b). Thus, the MPS thin films prepared using the P123 and F127 organic templates had XRD patterns with peaks in the 2θ range 1°–2° and a d spacing of 5–6 nm. After the removal of the polymers, the intensity of the peaks in the XRD patterns of these MPS thin films decreased. In addition, the films obtained via thermal treatment exhibited broader peaks in their XRD patterns than the VUV-treated films. This result indicates that polymer removal via VUV treatment occurred under milder conditions compared with those of thermal treatment, and resulted in the formation of relatively uniform pore arrays. Before and after the removal of the polymer, the decrease in the peak intensity and d-spacing occurred because of shrinkage of the silica framework, possibly resulting in the disruption of the pore arrays of the MPS thin films. The XRD intensity of the MPS thin films prepared using F127 significantly decreased after the removal of the polymer because the shrunken silica framework was not able to maintain the larger pore size.

Fig. 2 shows the contact angles of the MPS thin films (P123-FT and P123-FV). The contact angle of P123-FT and P123-FV were 18.8° and 3.1°, respectively. Silica-FN (dried at 80 °C for 3 h), F127-FT, and F127-FV were 31.9°, 28.9°, and 4.8°, respectively (Fig. S1). Clearly, the hydrophilic properties of the MPS thin films significantly increased after VUV treatment. This increase in the hydrophilicity was attributed to the exposure of Si – OH groups on the surface of the VUV-treated thin films, which might enable increased interaction with protein molecules. Importantly, the hydrophilic properties of the MPS thin films did not change, even after 5 days.

The results of the RMS roughness analyses are presented in Fig. 3 [38–42]. The values of the RMS roughness were found to be 0.664 nm and 0.783 nm for P123-FT and P123-FV, respectively. In addition, the values were 0.296 nm, 0.414 nm, and 0.664 nm for Silica-FT, F127-FT, and F127-FV (Fig. S2). The P123-FV thin film had a uniform pore array and the highest RMS roughness value, although the RMS roughness for F127-FV was similar to that of P123-FV. Notably, the F127-FT thin film was remarkably shrunken after the thermal treatment; therefore, its RMS roughness value was the lowest (0.414 nm) for all of the MPS thin films. The combined results of the XRD and DFM analyses revealed that the P123-FV thin film possessed the most uniform mesoporous structure. In addition, the thickness of the P123-FV film was 131.34 nm, and the voids in the film accounted for 39% of the film areas as measured using an ellipsometer. This thickness is similar to that of previously described films [43].

3.2. Adsorption of protein A and IgG on the MPS thin films

Next, protein A adsorption on the MPS thins films was evaluated, and it was found that 158 ng (protein A)/mm^2, 176 ng/mm^2, 125 ng/mm^2, 180 ng/mm^2, and 123 ng/mm^2 were adsorbed onto the Silica-FN, P123-FT, P123-FV, F127-FT, and F127-FV films, respectively (Fig. 4a). Interestingly, the amount of adsorbed protein A on both of the VUV-treated films was slightly lower than that absorbed on the corresponding thermally treated films. Because the molecular size of protein A is approximately 3 nm [7] and the pore size of the MPS thin films is approximately 5 nm, protein A was trapped in the pores of the films. Similar amounts of protein A were entrapped on the P123-FT and F127-FT films, which had nonuniform porous structures. Interestingly, protein A adsorption was also observed on Silica-FN, which has a flat silica surface with no mesopores. These results suggest that protein A is trapped in not only the interior of the pores but also the silica framework. Protein adsorption on the P123-FV MPS thin film was confirmed using DFM, and the results are presented in Fig. 5 and Table 1 [40,41,43].

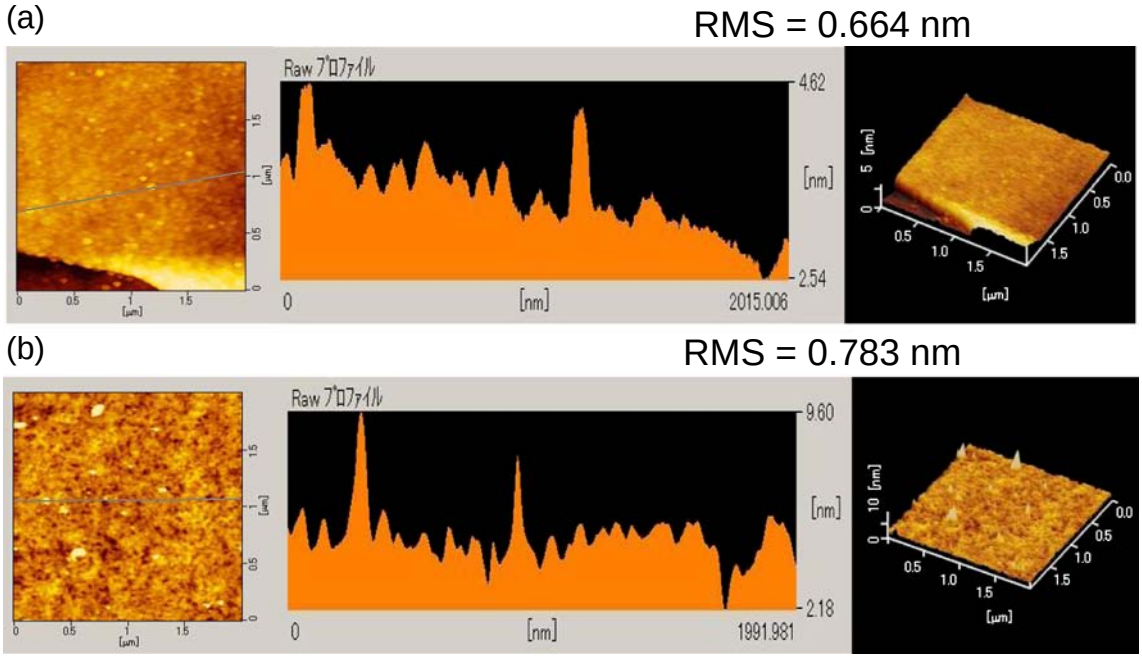

Fig. 3. Dynamic force microscopy (DFM) images and root mean square (RMS) roughness of mesoporous silica (MPS) thin films prepared via vacuum ultraviolet (VUV) and thermal treatment. (a) P123-FT and (b) P123-FV.

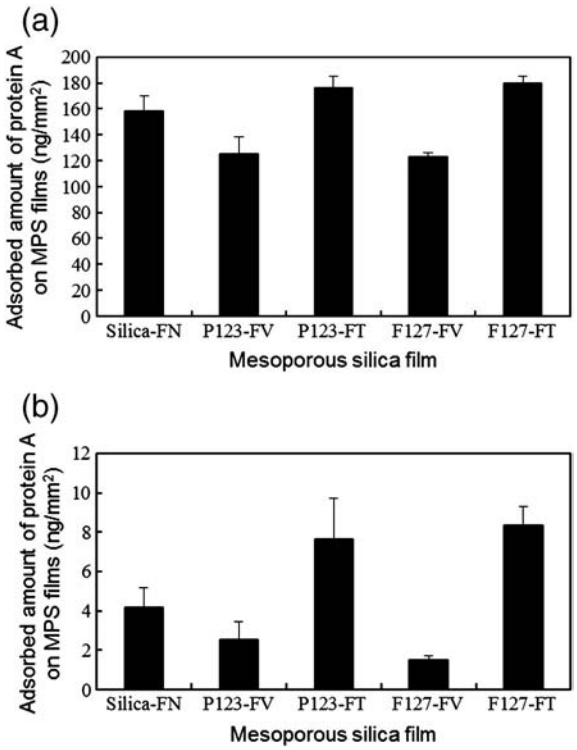

Fig. 4. Amount of (a) protein A adsorbed and (b) IgG bound to protein A adsorbed on mesoporous silica (MPS) thin films.

Because protein A reacts with the Fc fragment region of IgG from most mammalian species, it has been used extensively for quantitative and qualitative immunological techniques. Therefore, the specific adsorption of IgG for protein A adsorbed on the MPS thin films was investigated. The RMS roughness of an MPS thin film (P123-FV) before protein adsorption, after protein A adsorption, and after protein A–IgG binding were 0.78, 1.21, and 3.55 nm, respectively. In addition, the vertical distance increased from 4.06 to 19.48 nm, and the RMS roughness of the thin film after protein A–IgG binding also increased compared with the values obtained after protein A adsorption only (Table 1). The sizes of protein A and IgG are approximately 3 nm and 10 nm, respectively, and thus the change in the vertical distance corresponds to the addition of the size of each of these species. These results indicate that the IgG was adsorbed in a relatively uniform fashion on the protein A adsorbed on the P123-FV film.

The amount of IgG bound to protein A on the Silica-FN, P123-FT, P123-FV, F127-FT, and F127-FV films was then evaluated and determined to be 4.18 ng/mm^2, 7.65 ng/mm^2, 2.52 ng/mm^2, 8.33 ng/mm^2, and 1.48 ng/mm^2, respectively (Fig. 4b). The theoretical binding efficiency for protein A and IgG is 1:4, thus the efficiency of the MPS thin films was extremely low. This significant decrease in the binding efficiency is possibly due to the steric bulk of IgG. The size and molecular weight of IgG are approximately 10 nm and 15 kDa, respectively [44], and thus IgG may not be able to specifically adsorb onto all of the adsorbed protein A on the thin films. Furthermore, Fig. 4b clearly indicates that the amount of adsorbed IgG bound to protein A on the VUV-treated thin films was lower than that bound to protein A on the thermally treated films. In addition, no nonspecific binding of IgG was observed on the films without protein A. Improvement in the binding of IgG on the thermally treated films is attributed to the difference in binding environment for the two types of films. On the VUV-treated thin films (-FV films), IgG was only able to react vertically with protein A, while on the thermally treated thin films (-FT films), IgG could bind to protein A both horizontally and diagonally. A proposed model for protein A–IgG binding on the two differently treated films is shown in Scheme S2.

Next, protein adsorption and IgG binding on P123 MPS thin films was estimated by obtaining the nitrogen adsorption–desorption isotherms and pore size distributions of Santa Barbara amorphous (SBA) mesoporous silica particles prepared from a sol solution containing P123 as a substitute for the MPS thin films [7,44–46]. The nitrogen adsorption–desorption isotherms and pore size distributions of the SBA particles, SBA particles with adsorbed protein A, and SBA particles with adsorbed IgG–protein A complex are shown in Fig. S3. The figure clearly indicates that the quantity of nitrogen adsorbed (Fig. S3a) and the pore volume (Fig. S3b) decreased after protein A adsorption and following protein A–IgG binding on the SBA particles. These results suggest that protein A and IgG are located inside the mesopores. This phenomenon is also expected to occur on MPS thin films.

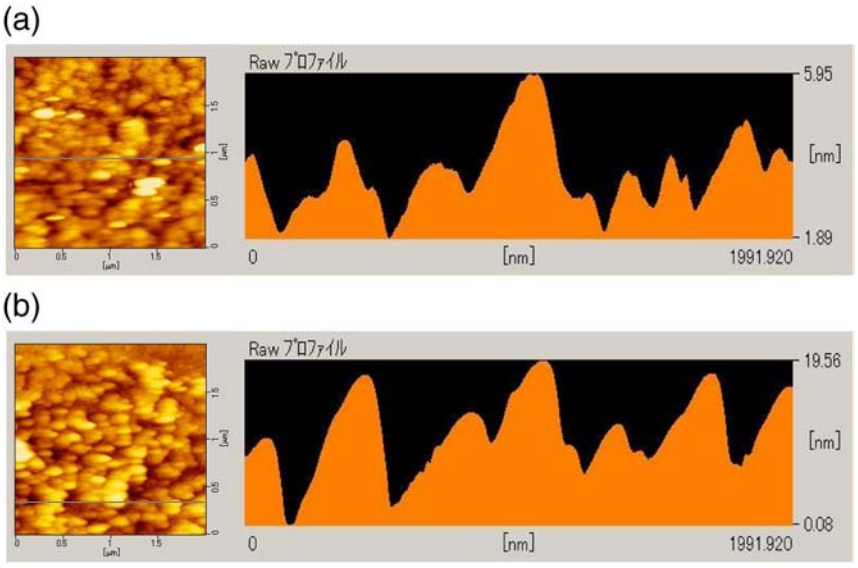

Fig. 5. Dynamic force microscopy (DFM) images of protein adsorption on mesoporous silica (MPS) thin films/(a) after protein A adsorption and (b) after protein A–IgG binding.

Table 1
Root mean square (RMS) and vertical distance of adsorbed protein on a mesoporous silica (MPS) thin film (P123-FV).

	Before protein adsorption	After protein A adsorption	After protein A–IgG binding
RMS (nm)	0.78 ± 0.22	1.21 ± 0.36	3.55 ± 1.22
Vertical distance (nm)		4.06 ± 1.53	19.48 ± 6.51

Based on the above results, Silica-FN, P123-FV, and P123-FT were used for further analysis because the P123 thin films had well-ordered mesopores compared with the F127 thin films.

3.3. ELISA on the MPS thin films

ELISA is a popular format for analytical biochemistry assays that detect the presence of a substance such as an antigen or antibody in a liquid or a wet sample. Therefore, ELISA tests on the MPS thin films were investigated in order to determine the potential of the films for use as highly sensitive biosensor platforms. The results for the determination of the ELISA sensitivity are presented in Fig. 6. The P123-FV thin film exhibited the highest sensitivity, while the Silica-FT and P123-FT thin films gave similar results. The highest ELISA sensitivity on the P123-FV thin film was due to the uniform pore array (Schemes S1 and S2a). This uniform array of IgG as the primary antibody may give rise to a highly effective antigen–antibody reaction, which would lead to the high ELISA sensitivity.

3.4. Catalytic activity of cyt c adsorbed on the MPS thin films

Next, cyt c was applied to the MPS thin film platform in order to expand the potential applications of the MPS thin film as an attractive platform for the preparation of biosensing systems. The amount of cyt c adsorbed on the P123-FV, P123-FT, and Silica-FN films was approximately 200 ng/mm^2 (data not shown). The higher levels of cyt c adsorption on the MPS thin films compared with that observed for protein A (Fig. 4) is due to the smaller molecular size (2 nm) of cyt c compared with that of protein A (3 nm).

The results for the specific activity of free cyt c and cyt c adsorbed on the P123-FV, P123-FT, and Silica-FN films are shown in Fig. 7a. It can be clearly seen that the specific activity (Abs/min/mg) of the cyt c adsorbed on the MPS thin films (0.030) was greatly decreased compared with that of the free cyt c solution (0.119). This decrease in the specific activity may be due to a lower diffusion efficiency of substrate compared with the cyt c adsorbed on the films. The recyclability of the cyt c adsorbed on the MPS thin films was also evaluated, and the relative activity of cyt c adsorbed on the films for up to six cycles is shown in Fig. 7b. The activity of the cyt c remaining on the P123-FV, P123-FT, and Silica-FN was approximately 60%, 21%, and 25%, respectively, after six cycles. The higher retention of catalytic activity for the cyt c on the P123-FV film is attributed to the uniform pore array. On the other hand, cyt c was not strongly immobilized on the P123-FT and Silica-FN thin films, which do not have ordered mesoporous structures. Specifically, a higher quantity of cyt c was released from the P123-FT and Silica-FN thin films after the catalytic reactions. Based on these results, it was concluded that the significant decrease in the catalytic activity after several cycles was due to the easy desorption of the cyt c from the P123-FT and Silica-FN thin films. This result suggests that the P123-FV thin film is suitable for application as a biosensor platform.

4. Conclusion

MPS thin films were prepared from sol–gel solutions using a spin-coating method, and films with uniform pore arrays were produced via VUV treatment for the removal of the triblock copolymer templates P123 and F127, while calcination at 500 °C provided nonuniform mesopore structures. The MPS thin film prepared using P123 as an organic template followed by VUV treatment (P123-FV) possessed the most uniform pore array. Application of the MPS thin films as biosensors was then investigated by conducting ELISA tests and evaluating the catalytic activity of cyt c on the MPS thin films. A highly effective antigen–antibody reaction on the P123-FV film led to the high ELISA sensitivity. Cyt c on the P123-FV thin film was also shown to exhibit catalytic activity, and the MPS film could be recycled. In summary, the P123-FV thin film prepared in this study has the potential for use in highly sensitive biosensors for the detection of tumor markers, the quantitation of endocrine disrupters, and so on.

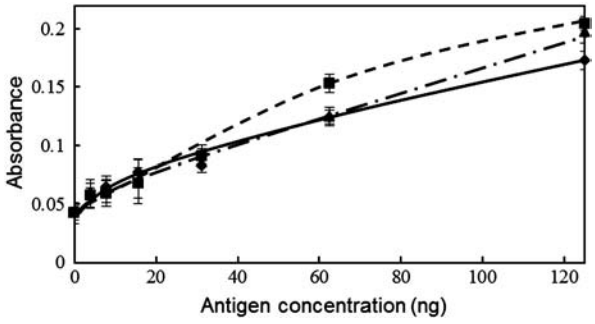

Fig. 6. Profiles of the enzyme-linked immunosorbent assay (ELISA) sensitivity of the mesoporous silica (MPS) thin films. Symbols: rhombus (♦): Silica-FN; square (■): P123-FV; triangle (▲): P123-FT.

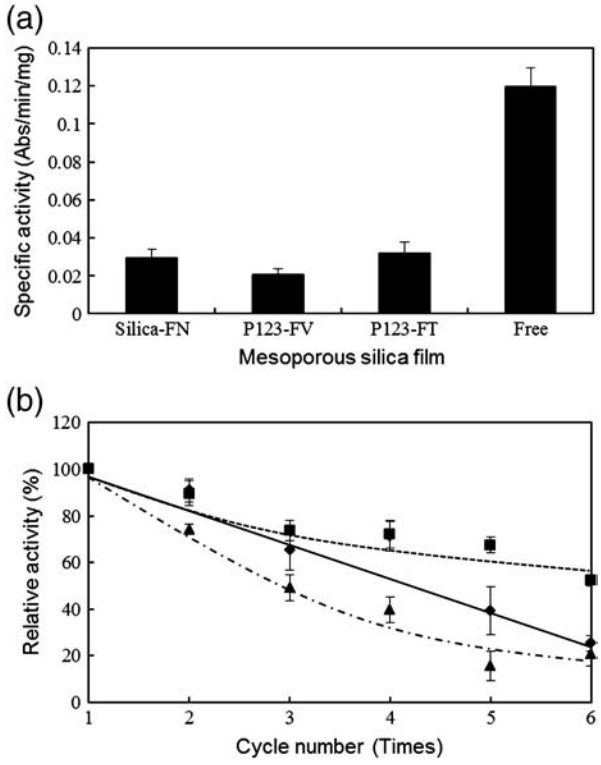

Fig. 7. Specific activity (a) and recyclability (b) of cytochrome c adsorbed on the mesoporous silica (MPS) thin films. Symbols: rhombus (♦): Silica-FN; square (■): P123-FV; triangle (▲): P123-FT.

Acknowledgments

K. K. thanks Dr. Atsushi Hozumi of the National Institute of Advanced Industrial Science and Technology (AIST) for his valuable information about VUV calcination of mesoporous silica films.

Appendix A. Supplementary data

Supplementary data to this article can be found online at http://dx.doi.org/10.1016/j.msec.2014.03.045.

References

[1] T. Yanagisawa, T. Shimizu, K. Kuroda, C. Kato, Bull. Chem. Soc. Jpn. 63 (1990) 988–992.
[2] S. Inagaki, Y. Fukushima, K. Kuroda, J. Chem. Soc. Chem. Commun. 8 (1993) 680–682.
[3] J.S. Beck, J.C. Vartuli, W.J. Roth, M.E. Leonowicz, C.T. Kresge, K.D. Schmitt, C.T.-W. Chu, D.H. Olson, E.W. Sheppard, S.B. McCullen, J.B. Higgins, J.L. Schlenkert, J. Am. Chem. Soc. 114 (1992) 10834–10843.
[4] Y. Ren, Z. Ma, P.G. Bruce, Chem. Soc. Rev. 41 (2012) 4909–4927.
[5] L. Zhao, H. Qin, R. Wu, H. Zou, J. Chromatogr. A 1228 (2012) 193–204.
[6] Y. Masuda, S. Kugimiya, K. Murai, A. Hayashi, K. Kato, Colloids Surf. B: Biointerfaces 101 (2013) 26–33.
[7] K. Nakanishi, M. Tomita, H. Nakamura, K. Kato, J. Mater. Chem. B 1 (2013) 6321–6328.
[8] M. Yang, H. Li, A. Javadi, S. Gong, Biomaterials 31 (2010) 3281–3286.
[9] M.G. Bellino, A.E. Regazzon, G.A.A. Soler-Illia, ACS Appl. Mater. Interfaces 2 (2010) 360–365.
[10] J. Park, M. Suh, Y. Kwon, Microporous Mesoporous Mater. 127 (2010) 147–151.
[11] M. Suh, H.J. Lee, J.Y. Park, U.H. Lee, Y.U. Kwon, D.J. Kim, ChemPhysChem 9 (2008) 1402–1408.
[12] S. Kataoka, Y. Takeuchi, A. Harada, M. Yamada, A. Endo, Green Chem. 12 (2010) 331–337.
[13] S.J. Updike, G.P. Hicks, Nature 214 (1967) 986–988.
[14] L. Sua, W. Jiaa, C. Houb, Y. Leia, Biosens. Bioelectron. 26 (2011) 1788–1799.
[15] A. Leunga, P.M. Shankar, R. Mutharasan, Sensors Actuators B Chem. 125 (2007) 688–703.
[16] J.R. Windmiller, J. Wang, Electroanalysis 25 (2013) 29–46.
[17] A. Heller, B. Feldman, Chem. Rev. 108 (2008) 2482–2505.
[18] S.A. Chiappini, D.J. Kormes, M.C. Bonetto, N. Sacco, E. Corton, Sensors Actuators B Chem. 148 (2010) 103–109.
[19] M.E. Dumant, T.S. Cardillo, M.K. Hayes, F. Sherman, Mol. Cell. Biol. 11 (1991) 5487–5496.
[20] R. Vazquez-Duhalt, J. Mol. Catal. B Enzym. 7 (1999) 241–249.
[21] K.D. Wael, Q. Bashir, S.V. Vlierberghe, P. Dubruel, H.A. Heering, A. Adriaens, Bioelectrochemistry 83 (2012) 15–18.
[22] J. Wu, M. Xu, G.C. Zhao, Electrochem. Commun. 212 (2010) 175–177.
[23] X. Zhang, J. Wang, W. Wu, S. Qian, Y. Man, Electrochem. Commun. 9 (2007) 2098–2104.
[24] A. Zhu, Y. Tian, H. Liu, Y. Luo, Biomaterials 30 (2009) 3183–3188.
[25] C. Zheng, X. Xu, F. He, L. Li, B. Wu, G. Yu, Y. Liu, Langmuir 26 (2010) 16730–16736.
[26] P. Li, Y. Song, Q. Guo, J. Shi, L. Liu, Mater. Lett. 65 (2011) 2130–2132.
[27] A. Hozumi, D.F. Cheng, Mater. Chem. Phys. 129 (2011) 464–470.
[28] O. Dubreuil, J. Dewalque, G. Chene, F. Mathis, G. Spronck, D. Strivay, R. Cloots, C. Henrist, Microporous Mesoporous Mater. 145 (2011) 1–8.
[29] S. Jung, T. Ha, W. Seo, Y.S. Lim, S. Shin, H.H. Chom, H. Park, J. Electron. Mater. 40 (2011) 652–656.
[30] Y. Hu, Y. Peng, L. Brousseau, A. Bouamrani, X. Liu, M. Ferrari, Sci. China. Chem. 53 (2010) 2257–2264.
[31] D. Zheng, J.M. Aramini, G.T. Montelione, Protein Sci. 13 (2004) 549–554.
[32] M. Graille, E.A. Stura, A.L. Corper, B.J. Sutton, M.J. Taussig, J. Charbonnier, G.J. Silverman, Proc. Natl. Acad. Sci. U. S. A. 97 (2000) 5399–5404.
[33] P.M. Wolny, J.P. Spatz, R.P. Richter, Langmuir 26 (2010) 1029–1034.
[34] A. Varghese, O.K. Raina, G. Nagar, R. Garg, P.S. Banerjee, B.R. Maharana, J.D. Kollannur, Vet. Parasitol. 183 (2012) 382–385.
[35] L. Chen, Z. Zhang, P. Zhang, X. Zhang, A. Fu, Sensors Actuators B 155 (2011) 557–561.
[36] Z. Xu, H. Deng, X. Deng, J. Yang, Y. Jiang, D. Zeng, F. Huang, Y. Shen, H. Lei, H. Wang, Y. Sun, Food Chem. 131 (2012) 1569–1576.
[37] N.H. Kim, M.S. Jeong, S.Y. Choi, J.H. Kang, Bull. Korean Chem. Soc. 25 (2004) 1889–1892.
[38] M.H. Sorensen, J.J. Valle-Delgado, R.W. Corkery, M.W. Rutland, P.C. Alberius, Langmuir 24 (2008) 7024–7030.
[39] A. Kierys, W. Buda, J. Goworek, J. Porous. Mater. 17 (2010) 669–676.
[40] K. Awsiuk, A. Bernasik, M. Kitsara, A. Budkowski, P. Petrou, S. Kakabakos, S. Parauzner-Bechcicki, J. Rysz, I. Raptis, Colloids Surf. B: Biointerfaces 90 (2012) 159–168.
[41] N.E. Kyrland, Z. Drira, V.K. Yadavalli, Micron 43 (2012) 116–128.
[42] T. Clark, J.D. Ruiz Jr, H. Fan, C.J. Brinker, B.I. Swanson, A.N. Parikh, Chem. Mater. 12 (2000) 3879–3884.
[43] J. Gu, C.M. Yam, S. Li, C. Cai, J. Am. Chem. Soc. 126 (2004) 8098–8099.
[44] T. Orita, K. Kato, M. Tomita, J. Ceram. Soc. Jpn. 119 (2011) 238–245.
[45] X. Zhang, W. Wu, J. Wang, X. Tain, Appl. Surf. Sci 254 (2008) 2893–2899.
[46] M. Claesson, N.J. Cho, C.W. Frank, M. Andersson, Langmuir 26 (2010) 16630–16633